SELECTIVE ANGLE MEASUREMENTS FOR A 3D-AOA INSTRUMENTAL VARIABLE TMA ALGORITHM

Kutluyıl Doğançay and Reza Arablouei

School of Engineering, University of South Australia, Mawson Lakes, SA 5095, Australia

ABSTRACT

The method of instrumental variables has been successfully applied to pseudolinear estimation for angle-of-arrival target motion analysis (TMA). The objective of instrumental variables is to modify the normal equations of a biased least-squares estimator to make it asymptotically unbiased. The instrumental variable (IV) matrix, used in the modified normal equations, is required to be strongly correlated with the data matrix and uncorrelated with the noise in the measurement vector. At small SNR, the correlation between the IV matrix and the data matrix can become weak. The concept of selective angle measurements (SAM) overcomes this problem by allowing some rows of the IV matrix and data matrix to be identical. This paper demonstrates the effectiveness of SAM for a previously proposed 3D angle-only IV TMA algorithm. The performance improvement of SAM is verified by simulation examples.

Index Terms— Selective angle measurements, 3D target motion analysis, angle-of-arrival localization, instrumental variables.

1. INTRODUCTION

Tracking of radio emitters has found many applications in mobile user localization, asset localization, sensor networks and target tracking in electronic warfare, to name but a few. In this paper we consider the use of selective angle measurements (SAM) in 3D angle-only target motion analysis (TMA). The objective of angle-only 3D-TMA is to estimate the position, velocity and possibly acceleration of a target from its azimuth and elevation angle measurements collected by a moving observer (ownship).

Whilst the TMA problem has been studied extensively in the 2D plane, there is little work reported on the angle-only 3D-TMA problem. In [1] a 3D localization algorithm was derived using an orthogonal vector estimation approach [2], [3] to estimate the location of a stationary radio emitter from angle measurements. A 3D-pseudolinear estimator (3D-PLE) and its weighted instrumental variable (WIV) version were also presented and shown to provide much improved estimation performance close to the maximum likelihood estimator (MLE). For moving targets, [4] proposes a so-called 3D improved PLE (3D-IPLE) drawing on the MLE cost function approximation used in [5], as well as some trigonometric approximations. The resulting estimator is the 2D-PLE for the 2D-projection of the 3D-TMA problem concatenated with the 3D-orthogonal vector estimator derived in [1]. The bias performance of the resulting estimator is improved by employing the bias compensation method in [6] and the method of WIV [7]. A different approach resembling the PLE in [1] has been adopted in [8], resulting in a 2D-PLE for the xy-components of the target motion parameter vector and a linear least-squares solution for the z-component. The bias performance of this new 3D-PLE was improved by applying bias compensation and WIV only to the 2D-PLE part of the estimator. The poor performance of the 3D-WIV estimator in large noise was analysed. The method of SAM, originally developed for self-localization [9], was employed to improve the performance of the 3D-WIV estimator in low SNR situations.

In this paper we consider the application of SAM to the WIV estimator in [4]. It is shown via numerical simulations that the SAM estimator can improve the performance of this WIV estimator at large noise levels thanks to its assurance of strong correlation between the IV matrix and data matrix. Section 2 describes the 3D-TMA problem and sets out the assumptions made. Section 3 summarizes the MLE for 3D-TMA. An overview of the 3D-IPLE is provided in Section 4. Section 5 describes the method of SAM applied to the WIV estimator in [4]. Comparative simulation examples are presented in Section 6. The paper concludes in Section 7.

2. 3D-TARGET MOTION ANALYSIS PROBLEM

Fig. 1 depicts the 3D-TMA problem. The objective of 3D-TMA is to estimate the target location $\boldsymbol{p}_k$ from N noisy azimuth and elevation angle measurements taken at time instants $k \in \{0, 1, \ldots, N-1\}$. The angles are related to the target location $\boldsymbol{p}_k = [p_{x,k}, p_{y,k}, p_{z,k}]^T$ and observer location $\boldsymbol{r}_k = [r_{x,k}, r_{y,k}, r_{z,k}]^T$ through

$$\theta_k = \tan^{-1}\frac{\Delta y_k}{\Delta x_k}, \quad -\pi < \theta_k \leq \pi \tag{1a}$$

$$\phi_k = \sin^{-1}\frac{\Delta z_k}{\|\boldsymbol{s}_k\|}, \quad -\frac{\pi}{2} < \phi_k \leq \frac{\pi}{2}. \tag{1b}$$

978-0-9928626-3-3/15/$31.00 ©2015 IEEE

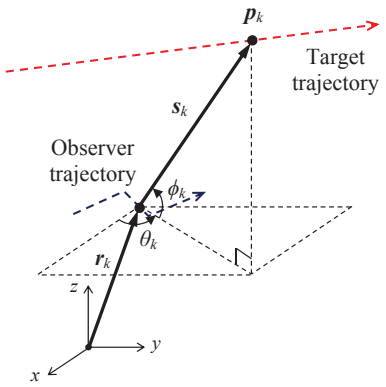

Fig. 1. 3D-TMA geometry using azimuth and elevation angles θ_k, ϕ_k.

Here $\tan^{-1}$ is the 4-quadrant arctangent,

$$\begin{aligned}\Delta x_k &= p_{x,k} - r_{x,k}\\ \Delta y_k &= p_{y,k} - r_{y,k}\\ \Delta z_k &= p_{z,k} - r_{z,k}\\ \boldsymbol{s}_k &= \boldsymbol{p}_k - \boldsymbol{r}_k\end{aligned}$$

and $\|\cdot\|$ denotes the Euclidean norm.

We make the following assumptions throughout the paper:

- The target moves with a constant velocity during the observation interval $k \in \{0, 1, \ldots, N-1\}$.
- The azimuth and elevation angle measurements are taken at regular time instants $t_k = kT/(N-1)$ where T is the length of the observation interval. Let $\boldsymbol{p}_0$ denote the initial target location vector at $k=0$ and $\boldsymbol{v}_0$ the constant velocity vector. Then the target location at time t_k is

$$\boldsymbol{p}_k = \boldsymbol{p}_0 + t_k \boldsymbol{v}_0 \tag{2a}$$
$$= \boldsymbol{M}_k\, \boldsymbol{\xi} \tag{2b}$$

  where

$$\boldsymbol{M}_k = \begin{bmatrix} 1 & 0 & 0 & t_k & 0 & 0\\ 0 & 1 & 0 & 0 & t_k & 0\\ 0 & 0 & 1 & 0 & 0 & t_k \end{bmatrix}$$

  and

$$\boldsymbol{\xi} = \begin{bmatrix} \boldsymbol{p}_0 \\ \boldsymbol{v}_0 \end{bmatrix}$$

  is the 6×1 *target motion parameter* vector to be estimated from noisy angle measurements. Given an estimate of target motion parameters $\hat{\boldsymbol{\xi}}$, $\boldsymbol{p}_k$ can be estimated by substituting $\hat{\boldsymbol{\xi}}$ for $\boldsymbol{\xi}$ in (2).
- The azimuth and elevation angle measurements are corrupted by independent zero-mean Gaussian noise:

$$\begin{aligned}\tilde{\theta}_k &= \theta_k + n_k, \quad n_k \sim \mathcal{N}(0, \sigma_{n_k}^2)\\ \tilde{\phi}_k &= \phi_k + m_k, \quad m_k \sim \mathcal{N}(0, \sigma_{m_k}^2)\end{aligned} \tag{3}$$

  where n_k and m_k are independent.
- The target is observable. This requires the observer to outmaneuver the target while collecting the angle measurements [10–13].

3. MAXIMUM LIKELIHOOD ESTIMATOR

Under the independent additive Gaussian noise assumption, the likelihood function for the angle measurements is

$$p(\tilde{\boldsymbol{\psi}}|\boldsymbol{\xi}) = \frac{1}{(2\pi)^N |\boldsymbol{K}|^{1/2}} \times \exp\Big\{-\frac{1}{2}(\tilde{\boldsymbol{\psi}} - \boldsymbol{\psi}(\boldsymbol{\xi}))^T \boldsymbol{K}^{-1} (\tilde{\boldsymbol{\psi}} - \boldsymbol{\psi}(\boldsymbol{\xi}))\Big\}$$

where

$$\tilde{\boldsymbol{\psi}} = [\tilde{\theta}_0, \tilde{\theta}_1, \ldots, \tilde{\theta}_{N-1}, \tilde{\phi}_0, \tilde{\phi}_1, \ldots, \tilde{\phi}_{N-1}]^T$$

is the $2N \times 1$ vector of noisy angle measurements,

$$\boldsymbol{\psi}(\boldsymbol{\xi}) = [\theta_0(\boldsymbol{\xi}), \theta_1(\boldsymbol{\xi}), \ldots, \theta_{N-1}(\boldsymbol{\xi}), \phi_0(\boldsymbol{\xi}), \phi_1(\boldsymbol{\xi}), \ldots, \phi_{N-1}(\boldsymbol{\xi})]^T$$

is the $2N \times 1$ vector of azimuth and elevation angles as a function of $\boldsymbol{\xi}$ with

$$\theta_k(\boldsymbol{\xi}) = \tan^{-1}\frac{\Delta y_k(\boldsymbol{\xi})}{\Delta x_k(\boldsymbol{\xi})}, \quad \phi_k(\boldsymbol{\xi}) = \sin^{-1}\frac{\Delta z_k(\boldsymbol{\xi})}{\|\boldsymbol{s}_k(\boldsymbol{\xi})\|} \tag{4}$$

and

$$\boldsymbol{s}_k(\boldsymbol{\xi}) = \begin{bmatrix} \Delta x_k(\boldsymbol{\xi}) \\ \Delta y_k(\boldsymbol{\xi}) \\ \Delta z_k(\boldsymbol{\xi}) \end{bmatrix} = \boldsymbol{M}_k\, \boldsymbol{\xi} - \boldsymbol{r}_k,$$

$\boldsymbol{K} = \mathrm{diag}(\sigma_{n_0}^2, \ldots, \sigma_{n_{N-1}}^2, \sigma_{m_0}^2, \ldots, \sigma_{m_{N-1}}^2)$ is the $2N \times 2N$ diagonal covariance matrix of the angle noise, and $|\boldsymbol{K}|$ denotes the determinant of $\boldsymbol{K}$.

The MLE of the target motion parameters $\hat{\boldsymbol{\xi}}_{\mathrm{ML}}$ is given by

$$\hat{\boldsymbol{\xi}}_{\mathrm{ML}} = \arg\min_{\boldsymbol{\xi}\in\mathbb{R}^6} J_{\mathrm{ML}}(\boldsymbol{\xi}) \tag{5}$$

where $J_{\mathrm{ML}}(\boldsymbol{\xi})$ is the ML cost function

$$J_{\mathrm{ML}}(\boldsymbol{\xi}) = \frac{1}{2}\boldsymbol{e}^T(\boldsymbol{\xi})\boldsymbol{K}^{-1}\boldsymbol{e}(\boldsymbol{\xi}), \quad \boldsymbol{e}(\boldsymbol{\xi}) = \tilde{\boldsymbol{\psi}} - \boldsymbol{\psi}(\boldsymbol{\xi}). \tag{6}$$

Equation (5) describes a nonlinear least squares estimator with no closed-form solution. A numerical solution can be obtained by using the Gauss-Newton (GN) algorithm:

$$\hat{\boldsymbol{\xi}}(i+1) = \hat{\boldsymbol{\xi}}(i) + (\boldsymbol{J}^T(i)\boldsymbol{K}^{-1}\boldsymbol{J}(i))^{-1}\boldsymbol{J}^T(i)\boldsymbol{K}^{-1}\boldsymbol{e}(\hat{\boldsymbol{\xi}}(i)), \quad i = 0, 1, \ldots \tag{7}$$

Here $\boldsymbol{J}(i)$ is the $2N \times 6$ Jacobian matrix of $\boldsymbol{\psi}(\boldsymbol{\xi})$ with respect to $\boldsymbol{\xi}$ evaluated at $\boldsymbol{\xi} = \hat{\boldsymbol{\xi}}(i)$:

$$\boldsymbol{J}(i) = -\begin{bmatrix} \frac{1}{\|\boldsymbol{s}_{xy,0}(\hat{\boldsymbol{\xi}}(i))\|}\boldsymbol{a}_0^T(\hat{\boldsymbol{\xi}}(i))\boldsymbol{M}_0 \\ \vdots \\ \frac{1}{\|\boldsymbol{s}_{xy,N-1}(\hat{\boldsymbol{\xi}}(i))\|}\boldsymbol{a}_{N-1}^T(\hat{\boldsymbol{\xi}}(i))\boldsymbol{M}_{N-1} \\ \frac{1}{\|\boldsymbol{s}_0(\hat{\boldsymbol{\xi}}(i))\|}\boldsymbol{b}_0^T(\hat{\boldsymbol{\xi}}(i))\boldsymbol{M}_0 \\ \vdots \\ \frac{1}{\|\boldsymbol{s}_{N-1}(\hat{\boldsymbol{\xi}}(i))\|}\boldsymbol{b}_{N-1}^T(\hat{\boldsymbol{\xi}}(i))\boldsymbol{M}_{N-1} \end{bmatrix} \tag{8}$$

where $\boldsymbol{a}_k(\hat{\boldsymbol{\xi}})$ is a unit vector orthogonal to the 2D-projection of the estimated 3D-range vector and $\boldsymbol{b}_k(\hat{\boldsymbol{\xi}})$ is a unit vector orthogonal to the estimated 3D range vector [1]:

$$\boldsymbol{a}_k(\hat{\boldsymbol{\xi}}(i)) = \begin{bmatrix} \sin\theta_k(\hat{\boldsymbol{\xi}}(i)) \\ -\cos\theta_k(\hat{\boldsymbol{\xi}}(i)) \\ 0 \end{bmatrix} \tag{9}$$

$$\boldsymbol{b}_k(\hat{\boldsymbol{\xi}}(i)) = \begin{bmatrix} \sin\phi_k(\hat{\boldsymbol{\xi}}(i))\cos\theta_k(\hat{\boldsymbol{\xi}}(i)) \\ \sin\phi_k(\hat{\boldsymbol{\xi}}(i))\sin\theta_k(\hat{\boldsymbol{\xi}}(i)) \\ -\cos\phi_k(\hat{\boldsymbol{\xi}}(i)) \end{bmatrix} \tag{10}$$

and

$$\boldsymbol{s}_{xy,k}(\boldsymbol{\xi}) = \begin{bmatrix} \Delta x_k(\boldsymbol{\xi}) \\ \Delta y_k(\boldsymbol{\xi}) \end{bmatrix}$$

is the projected range vector parameterized by $\boldsymbol{\xi}$.

Assuming *a priori* knowledge of the noise covariance matrix $\boldsymbol{K}$, the Cramer-Rao lower bound (CRLB) for the 3D-TMA problem is given by

$$\text{CRLB} = (\boldsymbol{J}_o^T\boldsymbol{K}^{-1}\boldsymbol{J}_o)^{-1} \tag{11}$$

where $\boldsymbol{J}_o$ is the Jacobian matrix evaluated at the true target motion parameter vector.

4. OVERVIEW OF 3D-IPLE

In [4] a matrix equation linear in $\boldsymbol{\xi}$ is obtained from a small-noise approximation of the MLE cost function following [5]. The resulting 3D-IPLE can also be derived by rewriting (1a) as

$$\frac{\sin(\tilde{\theta}_k - n_k)}{\cos(\tilde{\theta}_k - n_k)} = \frac{\Delta y_k}{\Delta x_k}$$

and lumping the noise terms together to get [14]

$$[\sin\tilde{\theta}_k, -\cos\tilde{\theta}_k, 0]\boldsymbol{M}_k\boldsymbol{\xi} = [\sin\tilde{\theta}_k, -\cos\tilde{\theta}_k, 0]\boldsymbol{r}_k + \eta_k \tag{12}$$

where $\eta_k = \|\boldsymbol{s}_k\|\cos\phi_k\sin n_k$, and rewriting (1b) as

$$\frac{\sin(\tilde{\phi}_k - m_k)}{\cos(\tilde{\phi}_k - m_k)} = \frac{\Delta z_k}{\|\boldsymbol{s}_{xy,k}\|}$$

or

$$\begin{aligned}&[\sin\tilde{\phi}_k\cos\tilde{\theta}_k, \sin\tilde{\phi}_k\sin\tilde{\theta}_k, -\cos\tilde{\phi}_k]\boldsymbol{M}_k\boldsymbol{\xi} \\ &\quad = [\sin\tilde{\phi}_k\cos\tilde{\theta}_k, \sin\tilde{\phi}_k\sin\tilde{\theta}_k, -\cos\tilde{\phi}_k]\boldsymbol{r}_k + \nu_k\end{aligned} \tag{13}$$

where $\nu_k = \|\boldsymbol{s}_k\|(\cos\phi_k\sin\tilde{\phi}_k\cos n_k - \cos\tilde{\phi}_k\sin\phi_k)$.

Stacking (12) and (13) for $k = 0, 1, \ldots, N-1$ gives

$$\boldsymbol{H}\boldsymbol{\xi} = \boldsymbol{d} + \boldsymbol{\omega} \tag{14}$$

where

$$\begin{aligned}\boldsymbol{H} &= [\boldsymbol{M}_0^T\boldsymbol{u}_0, \cdots, \boldsymbol{M}_{N-1}^T\boldsymbol{u}_{N-1}, \\ &\qquad \boldsymbol{M}_0^T\boldsymbol{v}_0, \cdots, \boldsymbol{M}_{N-1}^T\boldsymbol{v}_{N-1}]^T \\ \boldsymbol{d} &= [\boldsymbol{r}_0^T\boldsymbol{u}_0, \cdots, \boldsymbol{r}_{N-1}^T\boldsymbol{u}_{N-1}, \boldsymbol{r}_0^T\boldsymbol{v}_0, \cdots, \boldsymbol{r}_{N-1}^T\boldsymbol{v}_{N-1}]^T \\ \boldsymbol{\omega} &= [\eta_0, \cdots, \eta_{N-1}, \nu_0, \cdots, \nu_{N-1}]^T \\ \boldsymbol{u}_k &= [\sin\tilde{\theta}_k, -\cos\tilde{\theta}_k, 0]^T \\ \boldsymbol{v}_k &= [\sin\tilde{\phi}_k\cos\tilde{\theta}_k, \sin\tilde{\phi}_k\sin\tilde{\theta}_k, -\cos\tilde{\phi}_k]^T.\end{aligned}$$

We note that (14) is made up of two linear matrix equations concatenated; one for the 2D-PLE (projection of the 3D-TMA problem into the xy-plane) and the other for the orthogonal vector estimator [1].

The 3D-IPLE in [4] is the least-squares solution of (14):

$$\hat{\boldsymbol{\xi}}_{\text{IPLE}} = (\boldsymbol{H}^T\boldsymbol{H})^{-1}\boldsymbol{H}^T\boldsymbol{d}. \tag{15}$$

5. SELECTIVE ANGLE MEASUREMENTS

The correlation between $\boldsymbol{H}$ and $\boldsymbol{\omega}$ introduces undesirable estimation bias. Modifying the normal equations for the 3D-IPLE $\boldsymbol{H}^T\boldsymbol{H}\hat{\boldsymbol{\xi}}_{\text{IPLE}} = \boldsymbol{H}^T\boldsymbol{d}$ to $\boldsymbol{G}^T\boldsymbol{H}\hat{\boldsymbol{\xi}}_{\text{IV}} = \boldsymbol{G}^T\boldsymbol{d}$ gives the IV estimator:

$$\hat{\boldsymbol{\xi}}_{\text{IV}} = (\boldsymbol{G}^T\boldsymbol{H})^{-1}\boldsymbol{G}^T\boldsymbol{d}. \tag{16}$$

This estimate is asymptotically unbiased if $\boldsymbol{G}^T\boldsymbol{H}$ is full-rank and $E\{\boldsymbol{G}^T\boldsymbol{\omega}\} = \boldsymbol{0}$ [15]. An effective and simple method for constructing the IV matrix satisfying these requirements asymptotically was proposed in [7], which comprises the following steps:

- Obtain an initial estimate $\hat{\boldsymbol{\xi}}_{\text{IPLE}}$.
- Estimate the angles based on this initial estimate (cf. (4))

$$\hat{\theta}_k = \theta_k(\hat{\boldsymbol{\xi}}_{\text{IPLE}}), \quad \hat{\phi}_k = \phi_k(\hat{\boldsymbol{\xi}}_{\text{IPLE}}).$$

- Substitute the angle estimates for angle measurements in $\boldsymbol{H}$ to construct the IV matrix $\boldsymbol{G}$:

$$\boldsymbol{G} = \boldsymbol{H}|_{\tilde{\theta}_0=\hat{\theta}_0,\ldots,\tilde{\theta}_{N-1}=\hat{\theta}_{N-1},\tilde{\phi}_0=\hat{\phi}_0,\ldots,\tilde{\phi}_{N-1}=\hat{\phi}_{N-1}}.$$

Introducing a weighting matrix

$$\begin{aligned}\boldsymbol{W} = \boldsymbol{K}\,\text{diag}\Big(&\|\boldsymbol{s}_{xy,0}(\hat{\boldsymbol{\xi}}_{\text{IPLE}})\|^2, \cdots, \|\boldsymbol{s}_{xy,N-1}(\hat{\boldsymbol{\xi}}_{\text{IPLE}})\|^2, \\ &\big(\|\boldsymbol{s}_0(\hat{\boldsymbol{\xi}}_{\text{IPLE}})\|^2 - \|\boldsymbol{s}_{xy,0}(\hat{\boldsymbol{\xi}}_{\text{IPLE}})\|^2\sigma_{n_0}^2\big), \cdots, \\ &\big(\|\boldsymbol{s}_{N-1}(\hat{\boldsymbol{\xi}}_{\text{IPLE}})\|^2 - \|\boldsymbol{s}_{xy,N-1}(\hat{\boldsymbol{\xi}}_{\text{IPLE}})\|^2\sigma_{n_{N-1}}^2\big)\Big)\end{aligned}$$

results in a weighted IV estimator (3D-IWIV) [4]:

$$\hat{\boldsymbol{\xi}}_{\text{IWIV}} = (\boldsymbol{G}^T\boldsymbol{W}^{-1}\boldsymbol{H})^{-1}\boldsymbol{G}^T\boldsymbol{W}^{-1}\boldsymbol{d} \tag{17}$$

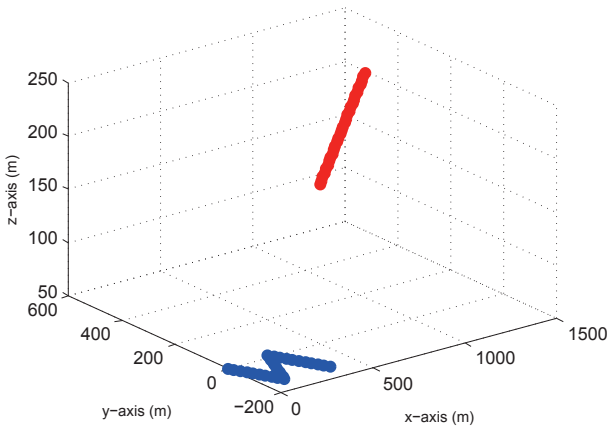

Fig. 2. Simulated 3D-TMA geometry.

which is asymptotically unbiased and efficient [16].

The matrices $\boldsymbol{G}$ and $\boldsymbol{H}$ are required to correlate well so that the product $\boldsymbol{G}^T\boldsymbol{H}$ is well-conditioned. If the unit vectors that make up these matrices do not align well as a result of large differences between $\hat{\theta}_k$ and $\tilde{\theta}_k$, and between $\hat{\phi}_k$ and $\tilde{\phi}_k$, the correlation between $\boldsymbol{G}$ and $\boldsymbol{H}$ can be weakened. This will increase the condition number of $\boldsymbol{G}^T\boldsymbol{H}$ and MSE. To avoid ill-conditioning of $\boldsymbol{G}^T\boldsymbol{H}$, some rows of the IV matrix can be forced to be identical to the corresponding rows of $\boldsymbol{H}$, depending on the difference between the angle estimates and measurements. This leads to the idea of SAM:

$$(\hat{\theta}_k, \hat{\phi}_k) = \begin{cases} (\hat{\theta}_k, \hat{\phi}_k) & \text{if } |\tilde{\theta}_k - \hat{\theta}_k| < \alpha_k \text{ and } |\tilde{\phi}_k - \hat{\phi}_k| < \beta_k \\ (\tilde{\theta}_k, \tilde{\phi}_k) & \text{otherwise.} \end{cases} \tag{18}$$

Here α_k and β_k are threshold values that should be chosen proportional to σ_{n_k} and σ_{m_k}, respectively. The angle estimates strongly influence the threshold values. The appropriate ranges for the thresholds are $2\sigma_{n_k} < \alpha_k < 5\sigma_{n_k}$ and $2\sigma_{m_k} < \beta_k < 5\sigma_{m_k}$.

The matrices $\boldsymbol{G}$ and $\boldsymbol{H}$ are maximally correlated if $\hat{\theta}_k = \tilde{\theta}_k$ and $\hat{\phi}_k = \tilde{\phi}_k$, $k = 0, 1, \ldots, N-1$, in $\boldsymbol{G}$. This amounts to replacing $\boldsymbol{G}$ with $\boldsymbol{H}$, which results in a least-squares estimator with severe bias problems. To retain some benefits of bias reduction, (18) offers a compromise solution. We will refer to the 3D-IWIV estimator employing (18) as the *3D-SAM-IWIV*. The performance improvement of SAM is determined by the reduction in the condition number of $\boldsymbol{G}^T\boldsymbol{W}^{-1}\boldsymbol{H}$. The relation of MSE performance to condition number will be demonstrated in the next section.

6. SIMULATIONS

The simulated TMA geometry is depicted in Fig. 2. The target moves with a constant velocity of $\boldsymbol{v}_0 = [60, 30, 1]^T$ m/s starting from an initial position $\boldsymbol{p}_0 = [500, 0, 200]^T$ m. The observer takes $N = 30$ angle measurements at regular time intervals ($t_{k+1} - t_k = 0.5$ s) while following a three-leg constant-velocity trajectory ($\boldsymbol{r}_0 = [0, 0, 50]^T$ m and the observer velocity alternates between $[25, -30, 0]$ m/s and $[25, 30, 0]$ m/s from one leg to another). The azimuth and elevation angle noise is i.i.d. with standard deviation σ.

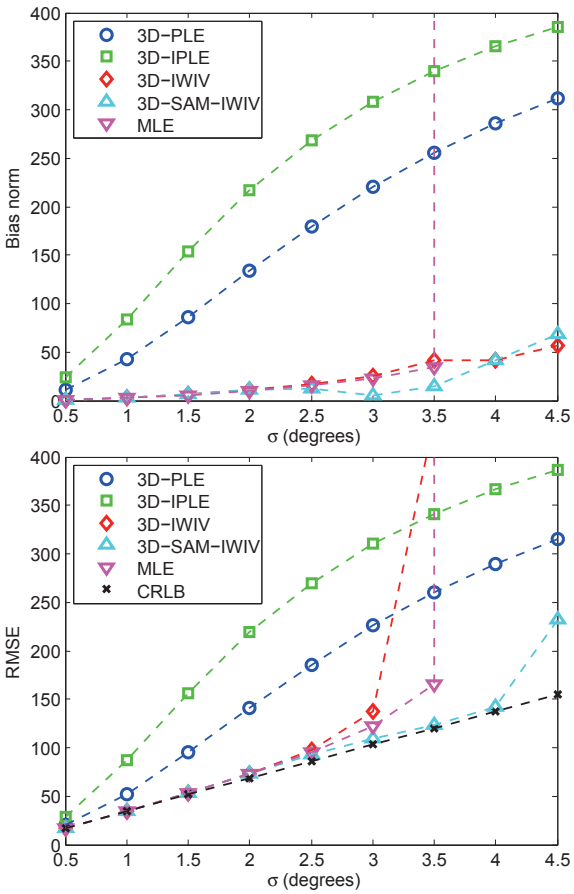

Fig. 3. Bias and RMSE performance.

The MLE is implemented using the GN algorithm, initialized to the 3D-IPLE and run for 10 iterations. The 3D-IWIV and 3D-SAM-IWIV estimators use the 3D-IPLE to construct the IV matrix $\boldsymbol{H}$ and the weighting matrix $\boldsymbol{W}$. For the 3D-SAM-IWIV estimator the threshold parameters are $\alpha_0 = \cdots = \alpha_{N-1} = 5\sigma$ and $\beta_0 = \cdots = \beta_{N-1} = 5\sigma$. All bias and RMSE values are estimated using 2,000 Monte Carlo simulation runs.

Fig. 3 shows the simulated bias norm and RMSE of the 3D-PLE in [8], 3D-IPLE, 3D-IWIV, 3D-SAM-IWIV and MLE. The RMSE plot also includes the CRLB (square root of trace of CRLB). For $\sigma > 3°$ both the 3D-IWIV and MLE exhibit a sharp increase in RMSE. This is due to the loss of correlation between $\boldsymbol{G}$ and $\boldsymbol{H}$ for the 3D-IWIV estimator and the threshold effect for the MLE. The 3D-SAM-IWIV avoids rapid deterioration of RMSE by assuring a strong correlation between $\boldsymbol{G}$ and $\boldsymbol{H}$. The method of SAM causes a nonvanishing residual correlation between the IV matrix and

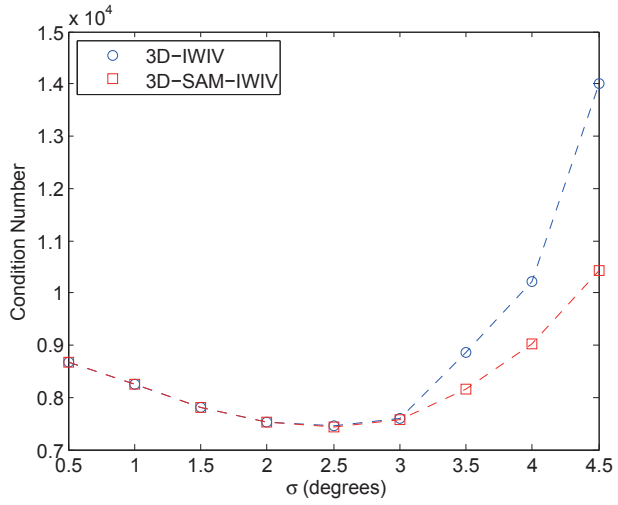

Fig. 4. Averaged condition number of $\boldsymbol{G}^T\boldsymbol{W}^{-1}\boldsymbol{H}$.

angle noise, which explains the slight degradation in the bias norm as the angle noise is increased. We also observe that the 3D-PLE [8] outperforms the 3D-IPLE [4] by a large margin.

In Fig. 4 the averaged condition numbers of $\boldsymbol{G}^T\boldsymbol{W}^{-1}\boldsymbol{H}$ for the 3D-IWIV and 3D-SAM-IWIV estimators are plotted against noise standard deviation. As the angle noise increases, the condition number of the 3D-IWIV significantly exceeds that of the 3D-SAM-IWIV, which demonstrates the effectiveness of SAM in maintaining a strong correlation between $\boldsymbol{G}$ and $\boldsymbol{H}$. This also explains the improved RMSE performance of the 3D-SAM-IWIV compared with 3D-IWIV (see Fig. 3).

7. CONCLUSION

The method of SAM has been applied to the 3D-IWIV proposed in [4]. The loss of correlation between the IV matrix $\boldsymbol{G}$ and the data matrix $\boldsymbol{H}$ was shown to impact the RMSE performance adversely. The effectiveness of SAM in combatting this loss was demonstrated by simulation examples. It was observed that both the RMSE performance and condition number of $\boldsymbol{G}^T\boldsymbol{W}^{-1}\boldsymbol{H}$ are significantly improved by employing SAM in the IV matrix.

REFERENCES

[1] K. Doğançay and G. Ibal, "Instrumental variable estimator for 3D bearings-only emitter localization," in *Proc. 2nd Int. Conf. on Intelligent Sensors, Sensor Networks and Information Processing, ISSNIP 2005*, Melbourne, Australia, December 2005, pp. 63–68.

[2] D. Koks, "Passive geolocation for multiple receivers with no initial state estimate," Tech. Rep. DSTO RR-0222, Defence Science & Technology Organisation, Edinburgh, SA, Australia, November 2001.

[3] K. Doğançay, "Bearings-only target localization using total least squares," *Signal Processing*, vol. 85, no. 9, pp. 1695–1710, September 2005.

[4] L. Badriasl and K. Doğançay, "Three-dimensional target motion analysis using azimuth/elevation angles," *IEEE Trans. on Aerospace and Electronic Systems*, vol. 50, no. 4, pp. 3178–3194, October 2014.

[5] M. Gavish and A. J. Weiss, "Performance analysis of bearing-only target location algorithms," *IEEE Trans. on Aerospace and Electronic Systems*, vol. 28, no. 3, pp. 817–828, 1992.

[6] K. Doğançay, "Bias compensation for the bearings-only pseudolinear target track estimator," *IEEE Trans. on Signal Processing*, vol. 54, no. 1, pp. 59–68, January 2006.

[7] K. Doğançay, "Passive emitter localization using weighted instrumental variables," *Signal Processing*, vol. 84, no. 3, pp. 487–497, March 2004.

[8] K. Doğançay, "3D pseudolinear target motion analysis from angle measurements," *IEEE Trans. on Signal Processing*, vol. 63, no. 6, pp. 1570–1580, March 2015.

[9] K. Doğançay, "Self-localization from landmark bearings using pseudolinear estimation techniques," *IEEE Trans. on Aerospace and Electronic Systems*, vol. 50, no. 3, pp. 2361–2368, July 2014.

[10] S. C. Nardone and V. J. Aidala, "Observability criteria for bearings-only target motion analysis," *IEEE Trans. on Aerospace and Electronic Systems*, vol. 17, pp. 162–166, March 1981.

[11] S. E. Hammel and V. J. Aidala, "Observability requirements for three-dimensional tracking via angle measurements," *IEEE Trans. on Aerospace and Electronic Systems*, vol. AES-21, no. 2, pp. 200–207, March 1985.

[12] J. M. Passerieux and D. Van Cappel, "Optimal observer maneuver for bearings-only tracking," *IEEE Trans. on Aerospace and Electronic Systems*, vol. 34, no. 3, pp. 777–788, July 1998.

[13] A. Farina, "Target tracking with bearings-only measurements," *Signal Processing*, vol. 78, pp. 61–78, 1999.

[14] A. G. Lindgren and K. F. Gong, "Position and velocity estimation via bearing observations," *IEEE Trans. on Aerospace and Electronic Systems*, vol. 14, no. 4, pp. 564–577, July 1978.

[15] L. Ljung, *System Identification: Theory for the User*, Prentice Hall, Upper Saddle River, NJ, 2 edition, 1999.

[16] K. Doğançay, "On the efficiency of a bearings-only instrumental variable estimator for target motion analysis," *Signal Processing*, vol. 85, no. 3, pp. 481–490, March 2005.